IEEE Access
Multidisciplinary ⋮ Rapid Review ⋮ Open Access Journal

Received December 10, 2020, accepted January 4, 2021, date of publication January 18, 2021, date of current version January 28, 2021.

Digital Object Identifier 10.1109/ACCESS.2021.3052517

Dielectric Performance of Silica-Filled Nanocomposites Based on Miscible (PP/PP-HI) and Immiscible (PP/EOC) Polymer Blends

XIAOZHEN HE[1], (Member, IEEE), PAOLO SERI[2], (Member, IEEE), ILKKA RYTÖLUOTO[3], RAFAL ANYSZKA[1], (Member, IEEE), AMIRHOSSEIN MAHTABANI[1], (Member, IEEE), HADI NADERIALLAF[2], (Member, IEEE), MINNA NIITTYMÄKI[4], (Graduate Student Member, IEEE), EETTA SAARIMÄKI[3], CHRISTELLE MAZEL[5], GABRIELE PEREGO[5], KARI LAHTI[4], (Member, IEEE), MIKA PAAJANEN[3], WILMA DIERKES[1], AND ANKE BLUME[1]

[1]Elastomer Technology and Engineering Group, Department of Mechanics of Solids, Surfaces & Systems (MS3), Faculty of Engineering Technology, University of Twente, 7522 NB Enschede, The Netherlands
[2]Department of Electrical, Electronic and Information Engineering "Guglielmo Marconi," University of Bologna, 40136 Bologna, Italy
[3]VTT Technical Research Center of Finland Ltd., 33101 Tampere, Finland
[4]High Voltage Engineering, Tampere University, 33720 Tampere, Finland
[5]Nexans Research Center, 69007 Lyon, France

Corresponding authors: Wilma Dierkes (w.k.dierkes@utwente.nl), Rafal Anyszka (r.p.anyszka@utwente.nl), and Xiaozhen He (x.he@utwente.nl)

This work was supported by the European Union's Horizon 2020 Research and Innovation Program under Grant 720858.

ABSTRACT This study compares different polymer-nanofiller blends concerning their suitability for application as insulating thermoplastic composites for High Voltage Direct Current (HVDC) cable application. Two polymer blends, PP/EOC (polypropylene/ethylene-octene copolymer) and PP/PP-HI (polypropylene/propylene - ethylene copolymer) and their nanocomposites filled with 2 wt.% of fumed silica modified with 3-aminopropyltriethoxysilane were studied. Morphology, thermal stability, crystallization behavior dynamic relaxation, conductivity, charge trap distribution and space charge behavior were studied respectively. The results showed that the comprehensive performance of the PP/PP-HI composite is better than the one of the PP/EOC composite due to better polymer miscibility and flexibility, as well as lower charging current density and space charge accumulation. Nanosilica addition improves the thermal stability and dielectric properties of both polymer blends. The filler acts as nucleating agent increasing the crystallization temperature, but decreasing the degree of crystallinity. Dynamic mechanical analysis results revealed three polymer relaxation transitions: PP glass transition (β), weak crystal reorientation ($\alpha 1$) and melting ($\alpha 2$). The nanosilica introduced deep traps in the polymer blends and suppressed space charge accumulation, but slightly increased the conductivity. A hypothesis for the correlation of charge trap distribution and polymer chain transition peaks is developed: In unfilled PP/EOC and PP/PP-HI matrices, charges are mostly located at the crystalline-amorphous interface, whereas in the filled PP/EOC/silica and PP/PP-HI /silica composites, charges are mostly located at the nanosilica-polymer interface. Overall, the PP/PP-HI (55/45) nanocomposite with 2 wt.% modified silica and 0.3 wt.% of antioxidants making it *a* promising material for PP based HVDC cable insulation application with *a* reduced space charge accumulation and good mechanical properties.

INDEX TERMS PP/EOC, PP/PP-HI, nanosilica, charge trap distribution, space charge accumulation, HVDC cable insulation.

The associate editor coordinating the review of this manuscript and approving it for publication was Guillaume Parent.

I. INTRODUCTION

High Voltage Direct Current (HVDC) technology shows advantages of lower dielectric losses and lower costs of long

distance power transmission in comparison to High Voltage Alternating Current (HVAC). The insulation material for cables plays an important role in the efficiency of power transmission in HVDC. Polypropylene (PP) as one of the possible insulation materials exhibits a relatively high melting temperature, recyclability and good dielectric properties. Therefore, it became an alternative insulation material to replace cross-linked polyethylene (XLPE) for HVDC cable applications recently [1]–[3]. However, PP exhibits low temperature brittleness, limiting its application for HVDC cables. To overcome this shortcoming, most studies for PP as insulation material nowadays are focused on PP-copolymers [4], [5] and PP/polyolefin blends [2], [6].

In PP-copolymers, a second monomer is copolymerized with propylene. It is reported that a polypropylene/polyethylene block copolymer is not a good choice for HVDC cable applications due to its brittleness and low elongation at break originating from the regular block-structure. Alternatively, a propylene/ethylene random copolymer exhibits superior low temperature elasticity, which are promising for HVDC applications [4].

Apart of PP-copolymerization, blending of PP with an elastomer can also improve the flexibility without compromising the electrical properties. Different types of polyolefins exhibiting elastomeric behavior can be used for this purpose. Some of them show limited miscibility with PP, even though they have a similar polymer composition [7], [8]. The type and content of the elastomer used for blending have been reported to influence morphology, crystallization, space charge accumulation and breakdown of the PP blend [6], [9]. As an example, C. D. Green and A. S. Vaughan [6] studied isotactic polypropylene/propylene-ethylene (with different ethylene content) blends. Polypropylene blends with 50 wt.% propylene-ethylene copolymer with an ethylene concentration of 9 mol% exhibited good electrical breakdown and mechanical properties on laboratory scale.

In the HVDC research field, space charge accumulation is one of the main concerns, since it can cause distortion of the local electric field resulting in partial discharge, and thus leading to insulation failure. [10] To solve this problem, PP based nanocomposites have drawn a lot of attention in both, industry and academia, due to the fact that a nanofiller can suppress space charge accumulation and charge trap distribution of an insulation material, which would enhance the electrical properties [11], [12]. In this study, we compared the different properties (morphology, thermal properties and dielectric performance) of two polymer composites based on polypropylene/propylene-ethylene copolymer and polypropylene/ethylene-octene copolymer blends and their nanocomposites in order to develop a promising insulation thermoplastic composite for HVDC cable application.

II. MATERIALS AND CHARACTERIZATIONS

A. MATERIALS

Fumed silica (Aerosil 200) was modified with 3-aminopropyltriethoxy silane (APTES) in a solvent-free reaction. 20 g of nanosilica was mixed with 3.6 g of APTES, 0.4 g of trifluoroacetic acid and 0.6 g of deionized water as catalysts in a sealed jar at room temperature for 24 hours. Then the modified silica was put into a vacuum oven at 80 °C for 24 hours in order to remove all unreacted residuals.

The nanocomposite samples were prepared by a Krauss-Maffei Berstorff ZE 25/49D twin screw extruder by melt-blending of 2 wt.% of the silica with PP/EOC = 55:45 wt.% or PP/PP-HI = 55:45 wt.% and 0.3 wt.% of antioxidants. The extruder set temperature ranges from 195 to 230 °C. The extruded compound was quenched in a water bath, granulated, and extruded into cast films by a single screw extruder (Brabender Plasticorder) equipped with a T die and a calendar system (80 °C). The average thickness of the cast film sample is around 400 μm.

B. SAMPLE CHARACTERIZATION

1) SCANNING ELECTRON MICROSCOPY (SEM)

Scanning Electron Microscopy (SEM) was performed on the samples in order to study the microstructure and silica dispersion using a Zeiss MERLIN HR-SEM (Oberkochen, Germany). The samples were firstly put into liquid nitrogen for 5 min and then broken into two parts. The cross section of these samples was selected for the SEM pictures without any surface treatment in order to preserve the surface morphology. The silica particle size distribution was obtained by ImageJ software by analyzing 3 SEM images of each compound.

2) X-RAY DIFFRACTION (XRD)

X-ray Diffraction (XRD) measurements were carried out on the plain samples with a Philips X'Pert 1 X-ray diffractometer (Almelo, The Netherlands). The samples were scanned from $2\Theta = 5°$ to 35° with a scanning rate of 0.05°/8 seconds.

3) DIFFERENTIAL SCANNING CALORIMETRY (DSC)

Differential Scanning Calorimetry (DSC) measurements were performed on the samples with a weight of 12 to 14 mg using a DSC NETZSCH DSC 214 Polyma (Germany). The samples were firstly cooled down to −50 °C and then heated up to 250 °C with a heating rate of 3 °C/min.

4) POLARIZED OPTICAL MICROSCOPE (POM)

Polarized light microscopy (POM, Meiji Techno ML8530 microscope) was done on the microtomed samples with a thickness of 30 μm.

5) THERMOGRAVIMETRIC ANALYSIS (TGA)

The thermal stability of the studied samples was investigated by Thermogravimetric Analysis (TA Instruments 550, US). The samples were heated up from 30 °C to 850 °C with a heating rate of 10 °C/min in synthetic air atmosphere.

6) DYNAMIC MECHANICAL ANALYSIS (DMA)

Dynamic Mechanical Analysis (DMA) tests were performed on an Eplexor 2000 N (Gabo/Netzsch, Germany) in tensile

mode with a frequency of 1 Hz; the static strain was 0.2 % and the dynamic strain was 0.1%. The samples were firstly cooled down to −100 °C and then heated up to 150 °C with a heating rate of 2 °C/min.

7) THERMALLY STIMULATED DEPOLARIZATION CURRENT (TSDC)

The charge trap distribution was tested by Thermally Stimulated Depolarization Current (TSDC) measurements by using a custom made setup comprising of a high voltage DC source (Keithley 2290E-5), an electrometer (Keithley 6517B) and a Novocool temperature control system equipped with a shielded sample cell and a PT100 temperature sensor (accuracy ±0.1 °C). A gold layer of 100 nanometers (nm) was deposited on both sides of the specimen acting as circular electrodes. The samples were polarized at 70 °C for 20 min under a 3 kV/mm DC field. Then the samples were rapidly cooled down to -50 °C. Later on, the poling voltage was removed and the samples were short circuited. TSDC was then measured by heating the samples from -50 °C to 140 °C with a linear heating rate of 3 °C/min.

8) PULSED ELECTRO ACOUSTIC (PEA)

Space charge behavior was investigated by a Pulsed Electro-Acoustic (PEA) method with a custom made setup comprising a high voltage DC source (FUG HCN 35 - 20000), a PEA cell built in-house and an oscilloscope (Tektronix 3032). The samples were firstly placed in a vacuum oven for 72 hours at 60 °C and then tested at 60 °C under a 30 kV/mm electric field. The electric field was applied for 3 hours (10800 s) for poling, after which the depolarization phase was monitored for 1 hour.

9) CONDUCTIVITY

The final conductivity test was done on the samples under an electric field of 30 kV/mm and at a temperature of 60 °C with a custom made setup comprising a high voltage DC source (FUG HCN 35 – 35000), an electrometer (Keysight B2980A) and a conductivity measurement cell built in-house. The samples were pretreated with gold sputtered electrodes with a diameter of 26 mm and a guard ring.

III. RESULTS AND DISCUSSIONS

A. SCANNING ELECTRON MICROSCOPY (SEM)

The morphology of the polymer blends and nanocomposites was studied using SEM and is shown in Figure 1. PP and PP-HI are uniformly distributed with no noticeable phase separation, which indicates that PP and PP-HI are highly miscible. In contrast to this, there is a significant phase separation in the PP/EOC blend. These two phases are arranged in a layered structure with the smooth phase being PP and the rough phase EOC. This reveals that PP and EOC have a limited degree of miscibility, visibly lower than PP and PP-HI. This leads to formation of an interface between the two polymers in the PP/EOC blend due to phase separation.

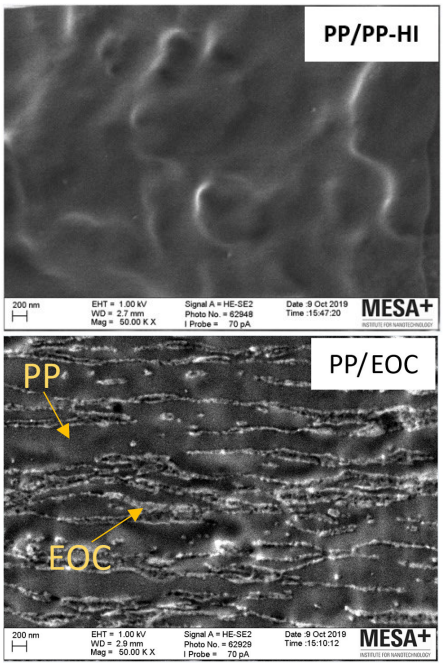

FIGURE 1. Morphology of the unfilled PP/EOC and PP/PP-HI composites.

The dispersion of the silica in the PP/EOC and PP/PP-HI matrices is shown in Figure 2. It is noticeable that the silica is distributed differently in the PP/EOC and PP/PP-HI matrices. The silica is evenly distributed in both phases in the PP/PP-HI matrix, while the silica incorporated into the PP/EOC matrix is located only in the PP phase. This effect occurs most likely because of a significant difference in the viscosity of PP and EOC. The PP chains of lower molecular weight (lower viscosity) exhibit higher mobility and thus can penetrate the porous structure of silica better than EOC, and therefore increase the PP/silica interaction favoring and stabilizing silica location in the PP phase. The preferential location of the silica in the PP phase is also confirmed by DSC, which will be discussed later. Furthermore, the histogram of the silica size distribution in both nanocomposites is shown in Figure 3. It is clearly seen that there are clusters of silica (> 100 nm) present in both, the PP/EOC and the PP/PP-HI matrix. This is due to the unpolar character of both polymer matrices, whereas the silica modified with 3-aminopropyltriethoxysilane has a polar character, which limits its dispersibility in the polymer matrices. Besides, there are relatively more large size silica clusters (>200 nm) present in the PP/EOC than in the PP/PP-HI matrix. This is caused by the preferred location of the silica in the PP phase of the PP/EOC matrix, which reduces the average distance between smaller silica clusters and thus a higher degree of recombination.

B. X-RAY DIFFRACTION (XRD)

In order to investigate the crystalline phase present in both blends and the nanocomposites, XRD was performed. The results are shown in Figure 4. In the left graph of Figure 4, only two peaks for pure EOC are found at 21.3° and 23.5°,

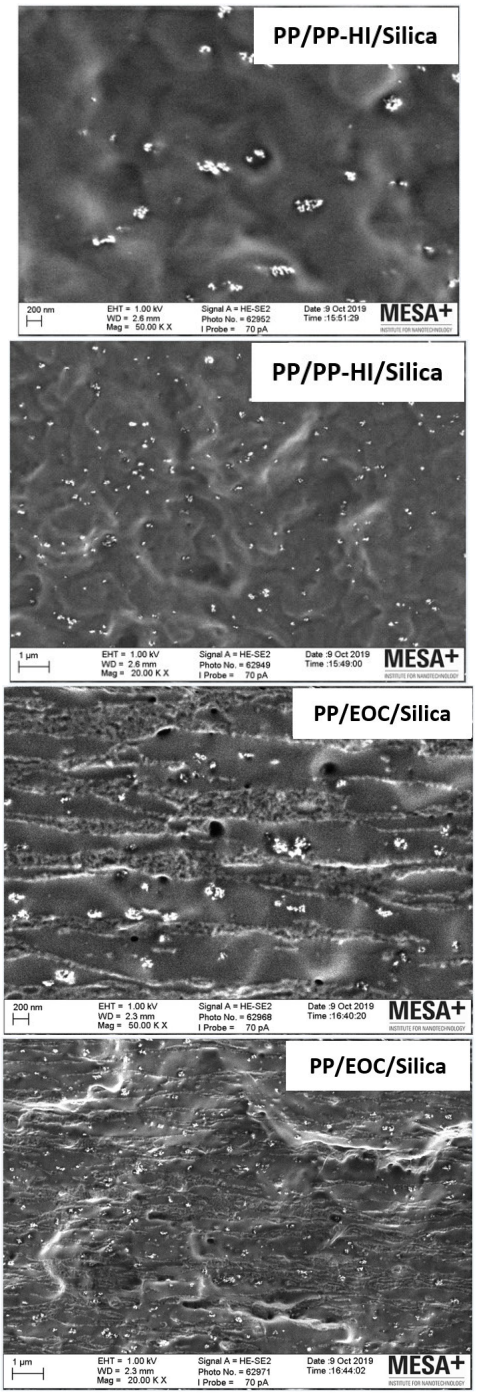

FIGURE 2. Morphology of silica-filled nanocomposites: PP/EOC/Silica and PP/PP-HI/Silica.

which are corresponding to the orthorhombic (110) and (200) crystal planes originating from polyethylene blocks present in the molecular structure of EOC, which are prone to crystallization. The same type of peaks for pure PP and pure PP-HI are found at similar positions corresponding to α-crystals formed by the PP phase. Peaks for the α-(110), α-(040), α-(130), α-(060) are located at $2\Theta = 14.1°$, $16.8°$, $18.5°$, $25.5°$ for pure PP, and at $2\Theta = 14.5°$, $17.2°$, $18.8°$, $25.6°$ for pure PP-HI, respectively. This indicates that PP and PP-HI

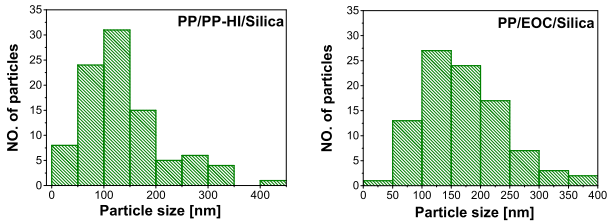

FIGURE 3. Silica particle size distribution in PP/EOC and PP/PP-HI matrix.

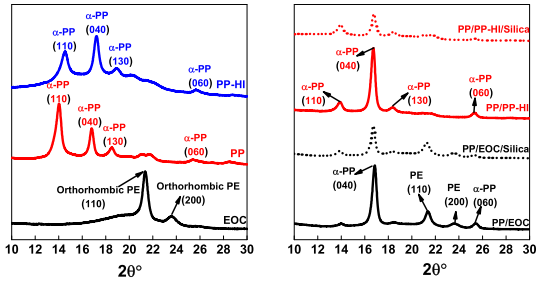

FIGURE 4. XRD results of pure PP, EOC and PP-HI (left), and PP/EOC, PP/PP-HI, PP/EOC/Silica, PP/PP-HI/Silica composites (right).

have a similar crystalline structure, while PP and EOC have different ones. When blending PP and PP-HI, the crystal peaks stemming from pure PP and PP-HI are invariable and all show up in the spectrum of the PP/PP-HI samples in the right graph of Figure 4. All peaks indicate α-crystals, from which the α-(040) structure is the most pronounced one. However, when mixing PP and EOC together, the α-(110) and α-(130) crystals almost disappear, while the α-(040) and α-(060) from the PP phase and the orthorhombic PE (110) and (200) from the EOC phase are found to be predominant. This shows that blending influences the morphology of the crystalline phase in both cases (PP/PP-HI and PP/EOC) promoting formation of the α-(040) structure over the α-(110) one.

Both nanocomposites show the same type of crystals as the unfilled polymer blends. However, it is clearly seen that the intensity of the peak is considerably reduced by adding silica, compared to the unfilled blends, revealing that the number of crystals is decreased by adding silica.

C. DIFFERENTIAL SCANNING CALORIMETRY (DSC)

The DSC thermograms (Figure 5) show the presence of two peaks of melting and crystallization of the PE and PP crystals in the unfilled PP/EOC blend and its nanocomposite. The crystallinity (Xc) was calculated and is presented in Table 1. The calculation is based on the Equation (1).

$$Xc\% = \frac{\Delta Hm}{w\Delta H100}100\% \quad (1)$$

where:

ΔHm - melting enthalpy of the sample,

w - weight percent of the polymer.

ΔH_{100} - melting enthalpy of the pure polymer.

In this equation, a ΔH_{100} value of 209 J/g is taken for PP [13] and 293 J/g for PE [14]

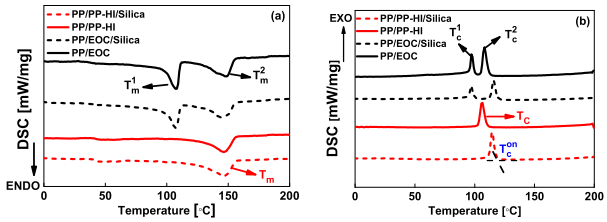

FIGURE 5. Melting (a) and crystallization (b) curves of PP/EOC, PP/PP-HI blends and PP/EOC/Silica, PP/PP-HI/Silica nanocomposites.

TABLE 1. Crystallization parameters.

	T_m^1 /°C	T_m^2 /°C	T_m /°C	T_c^1 /°C	T_c^2 /°C	T_c /°C	T_c^{on} /°C	Δ Hm / J/g	Δ X_C (%)
PP/EOC	107.2	147.2	-	97.2	108.2	-	114.2	-99.8	39.7
PP/EOC /Silica	106.3	146.3	-	97.3	116.3	-	120.2	-89.5	35.6
PP/PP-HI	-	-	146.1	-	-	105.5	112.0	-42.7	20.4
PP/PP-HI /Silica	-	-	146.2	-	-	114.2	118.3	-38.4	18.4

T_m^1 : melting peak temperature of the EOC phase;
T_m^2 : melting peak temperature of the PP phase;
T_m : melting peak temperature of the PP/PP-HI blend;
T_c^1 : crystallization peak temperature of the EOC phase;
T_c^2 : crystallization peak temperature of the PP phase;
T_c : crystallization peak temperature of the PP/PP-HI blend;
T_c^{on}: onset crystallization temperature;
Δ Hm: melting enthalpy of the polymer;
Δ X_c: calculated crystallinity of the polymer.

According to previous results [11], the two peaks belong to the EOC (Peak 1) and PP phase (Peak 2), respectively, while there is only one single peak observed in the PP/PP-HI blend and the PP/PP-HI/Silica composite. Moreover, we have seen that the onset crystallization temperature of the PP/EOC blend is higher than the one of the PP/PP-HI. This is caused by EOC acting as heterogeneous nucleating agent, accelerating the crystallization process in the PP/EOC blend [15]. The crystallinity of the PP/EOC blend is also higher than the one of the PP/PP-HI blend, as seen in Table 1.

Regarding the effect of silica addition as shown in Table 1, no significant melting temperature changes are observed after the incorporation of silica for any of the polymer blends. However, the incorporation of silica increased the crystallization temperature values by about 8 to 9 °C. This is due to the nucleation effect of the nanofiller [16]. For the PP/EOC based composite, two crystallization peaks are observed. The addition of silica has no influence on T_c^1, the crystallization peak temperature of the EOC phase, but increases the T_c^2 measured for the PP phase by about 8 °C. The different effects of silica in the two polymer matrices are a result of the distribution of silica: it is evenly distributed in the PP/PP-HI composite, while in the PP/EOC composite the silica is mostly located in the PP phase only. Therefore, the presence of silica changed only the T_c^2 of the PP phase, but has no effect on the T_c^1 of the EOC phase in the PP/EOC composite.

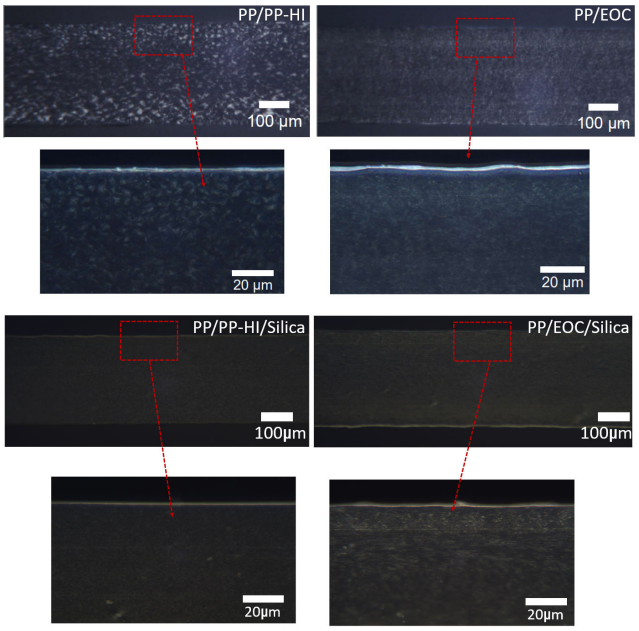

FIGURE 6. POM images of PP/EOC, PP/PP-HI blends and PP/EOC/Silica, PP/PP-HI/Silica nanocomposites.

It can be seen that the crystallinity of the unfilled PP/EOC blend is higher than the one of the unfilled PP/PP-HI blend. There is a significant reduction of crystallinity in both nanocomposites compared to the unfilled polymer blends [17]. When introducing silica into a polymer matrix, this brings about a large interface between silica and the polymer matrix. The interaction between silica and polymer decreases the chain mobility in the interface. This leads to lower chain mobility inhibiting crystallization and, as a consequence, less and smaller crystals are formed [18].

It is also interesting to note that silica increased the crystallization temperature (DSC results, Figure 5), but decreased the crystallinity of both polymer matrices (Table 1). Such a behavior was also observed by other authors [17]–[19]. This stems from the double function of nanosilica in a polymer matrix [18], [19]:

(i) Silica acts as a nucleating agent, which accelerates the process of non-isothermal crystallization.

(ii) The polymer interacts with the silica surface, the more as the surface area of the filler is rather large. This adsorption blocks the movement of crystallizable molecular chain segments and thus disturbs crystallization.

D. POLARIZED OPTICAL MICROSCOPE (POM)

Figure 6 shows the polarized light micrographs of the PP/EOC and PP/PP-HI blends as well as the PP/EOC/Silica and PP/PP-HI/Silica nanocomposites. For both unfilled blends, the size of the spherulites in the PP/PP-HI blend is bigger than in the PP/EOC samples. This results from a nucleating effect of the EOC [15] in the PP/EOC blend, as also seen in the DSC results in Figure 5, which will induce smaller spherulites. From the DSC results, it can be concluded that the crystallinity of the PP/EOC blend is higher than the

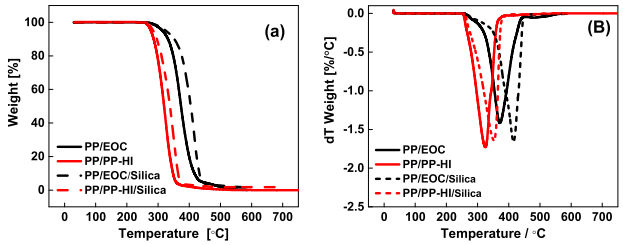

FIGURE 7. TGA profile (a) and the derivative (b) of PP/EOC, PP/PP-HI blends and PP/EOC/Silica, PP/PP-HI/Silica nanocomposites.

TABLE 2. Peak decomposition temperature T_D of PP/EOC, PP/PP-HI and PP/EOC/Silica, PP/PP-HI/Silica nanocomposites.

Sample	PP/EOC	PP/EOC/Silica	PP/PP-HI	PP/PP-HI/Silica
T_D / °C	370.4	416.4	324.2	350.7

one of PP/PP-HI. Higher crystallinity together with smaller crystals results in a larger amorphous-crystalline interface in the PP/EOC blend than in the PP/PP-HI blend. This difference in the amorphous-crystalline interface is expected to influence the dielectric properties, which will be discussed in Section 7 and 8.

The addition of nanosilica significantly decreases the spherulite size: no bright spherulites are visible in the POM images of the nanocomposites. Most likely that the crystal size of the spherulites is too small to be visible in the nanocomposites, especially in the one of PP/PP-HI/silica. This is in line with the DSC results, indicating that nanosilica acts as nucleating agent. Furthermore, we have observed that the presence of silica homogenized the distribution of the spherulites in the polymer, while for unfilled blends, the spherulites have different sizes and are not evenly distributed in the polymer (Figure 6). It is noticeable that there is also a difference in morphology between PP/PP-HI/silica and PP/EOC/silica. This is due to the effect of the different silica distribution and dispersion in both polymeric matrices. In case of PP/PP-HI/silica, the silica is evenly distributed in the polymer, leading to an uniformly distributed nucleating agent (silica) and evenly distributed spherulite. Differently, the silica is only located in PP phase in the sample of PP/EOC/silica, causing a heterogeneous distribution of spherulites. As it is known that the crystalline-amorphous area interfacial area affect the dielectric properties, the changes the spherulite size and distribution are expected to influence the dielectric properties.

E. THERMOGRAVIMETRIC ANALYSIS (TGA)

The thermal stability was studied by TGA in a synthetic air atmosphere. The mass loss kinetics recorded during heating are presented in the left graph of Figure 7, and their corresponding derivative (DTGA) results are shown in the right graph of the same figure. The peaks of the DTGA indicating the highest decomposition rate are given in Table 2.

During the thermal degradation, a single step degradation is obvious for all samples. Thermal decomposition of the unfilled PP/EOC blend occurs at higher temperatures than of the unfilled PP/PP-HI blend. This is possibly due to the higher thermal stability of EOC compared to polypropylene [20], that increases the overall thermal stability of the PP/EOC blend.

The incorporation of nanosilica causes a shift of the DTGA peak to a higher temperature in both polymer matrices, which indicates that nanosilica can improve their thermal stability. Analogous behavior has been reported in literature [21]–[24]. During the thermal degradation of PP, volatile hydrocarbon products are generated through a radical degradation process, and the weight loss is proportional to the amount of volatile products generated. The degradation mechanism is mainly based on chemical bond scission starting from the polymer chain ends. The same behavior is expected for the blends [22]. The role of a nanofiller in enhancing the thermal stability of the PP/PP-HI/Silica composite is ascribed to the weight loss retarding effect of a nanofiller: the volatile products (especially the polar volatiles and oxidized volatiles such as H_2O_2, ketons, alcohols) can be physically or chemically adsorbed onto the nanofiller surface, thus leading to their delayed release [25], resulting in an effective delay of mass loss described as improved thermal stability [21].

F. DYNAMIC MECHANICAL ANALYSIS (DMA)

The dynamic mechanical behavior was investigated by means of a DMA in order to verify the compatibility and dynamic transitions. The time dependence of the storage and loss modulus as well as the loss factor are shown in Figure 8.

The storage modulus (E′) is associated with the elastic energy stored in the polymer and influenced by polymer morphology changes, for example, by the crystalline phase [26]. The storage modulus E′ of PP/EOC is higher than the one of the PP/PP-HI blend, which is attributed to its higher crystallinity (Table 1): crystallites act as polymer network nodes and thus contribute to the reinforcement. The addition of nanosilica decreased the storage modulus of both polymer matrices, which is a direct consequence of the crystallinity reduction.

The loss modulus (E″) peak temperature ranges indicate the corresponding transition zones [27]. Figure 8 (b) shows, that there is a broad peak, Peak 1, between −80 °C and 150 °C, with the maximum around −5.7 °C in the PP/EOC as well as the PP/EOC/silica sample. In addition, there are two peaks noticed at −33.7 °C (Peak 2) and 50 °C (Peak 3), which are overlapping with the broad Peak 1. Peak 1 (at −5.7 °C) and Peak 2 (at −33.7 °C) are the glass transition peaks of the PP and EOC amorphous phase, respectively. The presence of these two peaks indicates that the miscibility between PP and EOC is low, which is corresponding to the conclusions based on the SEM pictures showing a co-continuous two-phase morphology. Peak 3 at 50 °C is attributed to melting of fragmentary crystals [28] and the molecular movements of the polyolefin with weak crystallization ability [29]. In the PP/PP-HI and PP/PP-HI/Silica samples, only one narrow and sharp Peak 4 is present around −22.7 °C, which proves

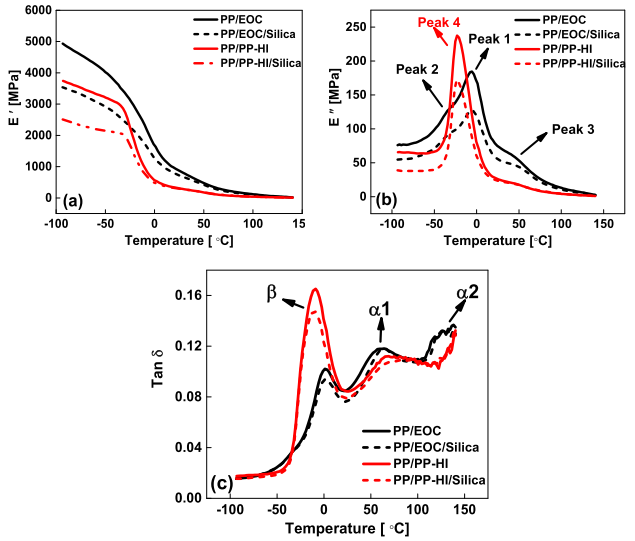

FIGURE 8. DMA curves of the PP/EOC, PP/PP-HI blends and PP/EOC/Silica, PP/PP-HI/Silica nanocomposites: (a) storage modulus vs temperature; (b) loss modulus vs temperature; (c) loss factor vs temperature.

that the miscibility between PP and PP-HI is high. In general, nanosilica addition has only a very slight effect on the dynamic transitions of polymers, but decreases the peak intensity of the loss modulus. This stems from the decreased crystallinity, which results in more mobile polymer chains in the amorphous phase.

The loss factor results from various polymer chain relaxation processes. All measured samples show three relaxation peaks: β, $\alpha 1$, $\alpha 2$. Addition of silica does not have any influence on these relaxation transitions. The β relaxation is associated with the relaxation of the amorphous polymer stemming from increased segmental movement of the macromolecules, which is also called glass transition [30]. The α relaxation [31] is associated with molecular motion within the crystals [32]. In our case, the $\alpha 1$ peak is related to the molecular motion within the weak crystals (imperfect crystal formation), and the $\alpha 2$ peak is caused by melting of the crystalline phase of the polymer blends.

G. THERMALLY STIMULATED DEPOLARIZATION CURRENT (TSDC)

Thermally Stimulated Depolarization Current (TSDC) measurements of the PP/EOC, PP/PP-HI blends and the PP/EOC/Silica, PP/PP-HI/Silica nanocomposites are shown in Figure 9. The charge trap level distribution curve is shown in the right graph of Figure 9. Comparing the unfilled PP/EOC and PP/PP-HI blends, both of them show one complete peak and one incomplete peak, associated with release of trapped charges. The position of the full peak at 55 °C of the PP/PP-HI sample is corresponding to a trap level of 0.98 eV, which is lower than the one of the PP/EOC sample (1.02 eV at 69 °C). The incomplete peaks of PP/PP-HI and PP/EOC are starting from a temperature of 93 °C and 100 °C, respectively, until the maximum measured temperature range.

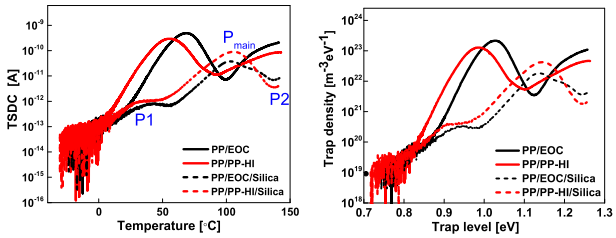

FIGURE 9. TSDC curve (left) and calculated trap level distribution (right) of the PP/EOC, PP/PP-HI blends and PP/EOC/Silica, PP/PP-HI/Silica nanocomposites.

The measured TSDC results also show that the depolarization current density of the unfilled PP/PP-HI sample is lower than the one of the unfilled PP/EOC sample. PP is a semi-crystalline polymer, with a large interface between the crystalline and amorphous phases. Due to the discontinuity at the interface between amorphous and crystalline areas, some chemical and/or physical disorder in chain alignment will be present at the interface, by which the charge carrier traps are formed [2]. It is reported that the interface between a crystalline and an amorphous phase is considered as the main factor for the formation of charge carrier traps [7], [33]. For the unfilled PP/PP-HI sample, crystallinity is lower (Table 1), but crystals are larger (Figure 5) compared to the PP/EOC sample, resulting in less interface area between the crystalline and amorphous phases in PP/PP-HI. Hence, the trap density of the PP/PP-HI sample is lower than the one of the PP/EOC sample. In addition, the interface between PP and EOC [34] resulting from their low miscibility may also contribute to the higher trap density in the PP/EOC sample compared to the homogenous PP/PP-HI sample. The higher main trap level of the unfilled PP/EOC blend (1.02 eV) compared to the level of the unfilled PP/PP-HI blend (0.98 eV) is probably due to the presence of the EOC phase. The separate phases formed by EOC and PP and the new type of crystals (orthorhombic PE (110) and PE (200)) introduced by the EOC phase creates physical and chemical disorder in the PP/EOC matrix. These physical and chemical disorders are defects, which act as charge traps. For these two unfilled blends, it is also interesting to note that the complete (P1) and the incomplete peak (P2) in the TSDC graph are corresponding to the $\alpha 1$ and $\alpha 2$ relaxation in the DMA results, respectively, as shown in Figure 10 (a) and (b). This indicates that the charge releasing process is associated with the α relaxation, which is the chain motion related to the constrained amorphous chain mobility and also the crystalline melting. It implies that the charges might mostly be located at the interface between crystalline and amorphous phases and intra-crystal areas in the unfilled blends, as shown in Figure 11.

In case of the nanocomposites, the addition of nanosilica significantly changes the trap distribution for both, PP/EOC and PP/PP-HI polymer matrices, as shown in Figure 8. There is one main peak (Pmain), one small peak P1 and one uncompleted peak P2 of the depolarization current, with a similar peak position for both, PP/EOC/Silica and PP/PP-HI/Silica nanocomposites. Moreover, there is no direct correlation

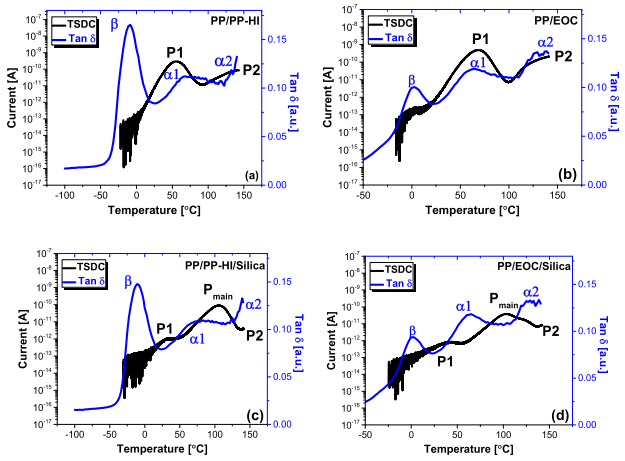

FIGURE 10. Correlation between TSDC depolarization current and DMA relaxation curve of unfilled PP/PP-HI (a), PP/EOC blend (b); PP/PP-HI/Silica (c); PP/EOC/Silica (d).

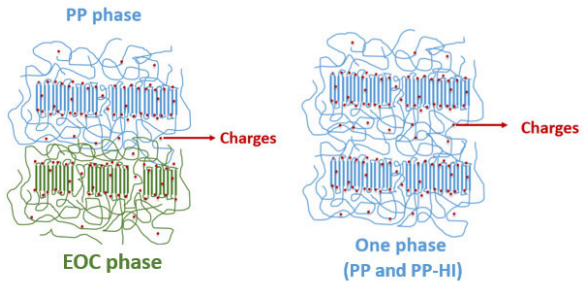

FIGURE 11. Schemes of the most of charges trapping site location in the PP/EOC blend (left) and PP/PP-HI blend (right) - the space between lamellae is filled with the amorphous polymer.

between the TSDC charge relaxation and DMA chain relaxation peaks, which is different from the unfilled blend.

Based on our previous study [35], we could conclude that addition of APTES modified silica can introduce a new deep trap level at 1.13 eV. It is identical with the trap location of Pmain at a trap level of 1.13 eV and 1.14 eV for the PP/EOC/Silica and PP/PP-HI/Silica nanocomposites, respectively. The nanosilica was modified by a silane containing a polar amine group, which brings new energy states into the composites, resulting in the deep trap formation (Pmain). The presence of the silica nanoparticles creates electrical defect centers inducing local electric fields, which further contribute to accumulation of the charge carriers at the filler-polymer interface [36]. Moreover, the interface between nanofiller and polymer matrix is considered to be the place of charge trap location [37]. Consequently, the newly introduced peak Pmain is most likely related to the interface between the silica and polymer matrix.

Peak P2 starts at a temperature of around 140 °C in both nanocomposites, and the trap level of this peak is above 1.25 eV. The appearance of P2 after silica incorporation was reported in literature [38], where the authors also found that addition of nanosilica introduces very deep charge traps at a temperature around 140-160 °C, which results from the silica itself acting as the deep traps. It is also reported that silanol groups and especially residual water molecules adsorbed on the silica surface exhibit strong attractive forces to electrons, withdrawing them from the polymer matrix [39]. As a consequence, the silica itself is able to create traps to attract charges; an indication that indeed silica itself created the deepest charge trap P2. However, in the current study, we have also noticed that:

1) The charge trap location of P2 around 140°C is the beginning of the melting process of PP in the PP/EOC and the PP/PP-HI blends;

2) The nanosilica in the PP/EOC blend is only located in the PP phase, and evenly distributed in the PP/PP-HI blend;

3) The nanosilica acts as nucleating agent and changes the crystal morphology (as shown in Figure 5) of both polymer blends. Therefore, it is reasonable to deduct that the P2 peak might stem from

a) the interface between nanosilica and the crystalline PP phase in PP/EOC/Silica and PP/PP-HI/Silica composites, or

b) the changed crystal morphology in both composites caused by the nanosilica.

The small peak P1 in the nanocomposites could be related to chain relaxation ($\alpha 1$) as shown in Figure 10, since they have similar starting temperature. It indicates that there might still be a little amount of charges, which are located at the interface between the amorphous and crystalline phases of the polymer. Due to the fact that the P1 peak intensity is much smaller than the one of Pmain, the nanosilica effect still dominates the charge relaxation process in the nanocomposites, with the nanofiller introducing deeper charge traps into the polymer blends. This is illustrated in Figures 11 and 12, in which the location of the trap sites is changed significantly due to the nanosilica incorporation.

In nanocomposites, the interface between nanofiller and polymer matrix is considered to be the main region of charge trap location [37]. In our nanocomposite, the trap density of Pmain in the PP/PP-HI/Silica composite is 4.39×10^{22} m^{-3} eV^{-1}, which is higher than the value of this peak in the PP/EOC/Silica composite (1.84×10^{22} m^{-3} eV^{-1}). This is related to micron-sized clusters of nanoparticles and the physical defects caused by them [40]. As seen in Figure 1, the nanosilica is mainly located in the PP phase in the PP/EOC/Silica composite, while it is evenly distributed in the PP/PP-HI/Silica composite. The PP/EOC and PP/PP-HI ratios are 55/45, therefore the silica in the PP/EOC blend has roughly only half the volume to be distributed in compared to the PP/PP-HI blend. The actual concentration of nanosilica in the PP phase is thus roughly two times higher in the former blend, resulting in lower filler-cluster distance and a stronger tendency to agglomerate in the PP/EOC/Silica system than in the PP/PP-HI/Silica composite. These larger silica units feature a relatively lower silica-polymer interface in the PP/EOC/Silica sample than in the PP/PP-HI/Silica sample.

There are two possible explanations for the much lower trap density of the nanocomposites in comparison to the unfilled blends:

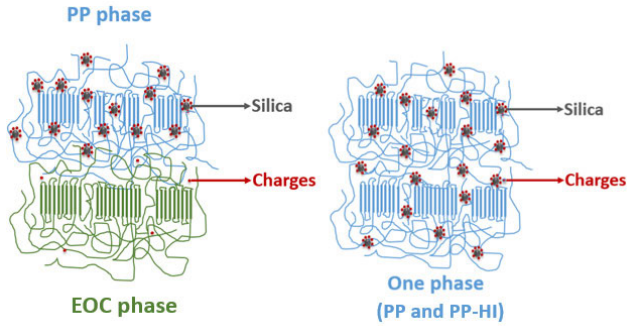

FIGURE 12. Schemes of the most of the charges trapping sites of the Pmain peak in the PP/EOC/Silica (left) and PP/PP-HI/Silica nanocomposites (right).

TABLE 3. The amount of space charge after Volt-off in the PP/EOC, PP/PP-HI blends and PP/EOC/Silica, PP/PP-HI/Silica nanocomposites.

Sample	PP/EOC	PP/EOC /Silica	PP/PP-HI	PP/PP-HI /Silica
Amount of space charge after Volt-off / C/m^3	3.3	1.5	2.7	0.6

1) The interface area between the nanosilica and polymer matrix is smaller than the interface between the crystalline and amorphous phase in the unfilled composites;

2) The deep traps introduced in the nanocomposites by the addition of silica immobilize charges. Consequently, the traps create a local electric field during poling inhibiting further charge injection, which leads to less injected charges in nanocomposites. As a result, lower TSDC values are measured and lower charge trap densities are calculated in both nanocomposites in comparison to the unfilled blends.

H. PULSED ELECTRO ACOUSTIC (PEA) ANALYSIS

To further investigate the space charge accumulation, PEA tests were performed. Space charge patterns of all samples are shown in Figure 13. The red and blue color represent the positive and negative charge densities, respectively. The upper electrode corresponds to the anode, while the lower is the cathode. Color bars represent the scale of charge density. The horizontal axis represents time (both polarization and depolarization) in seconds (s), the vertical axis represents the thickness of the tested sample in meters (m). The amount of space charge detected immediately after the beginning of the depolarization phase (Volt-off) is shown in Table 3. For the unfilled blends, the charge packets travel through the test specimens. However, it is obvious that the PP/PP-HI blend exhibited a lower amount of heterocharge (charge with opposite polarity to the electrode it is closer to) than PP/EOC. Table 3 also shows that the space charge accumulation for PP/PP-HI is lower than for PP/EOC. This might be due to the low compatibility between PP and EOC resulting in the generation of physical defects in the PP/EOC matrix [41]. Besides, the depth of the unfilled PP/EOC (1.02 eV) is

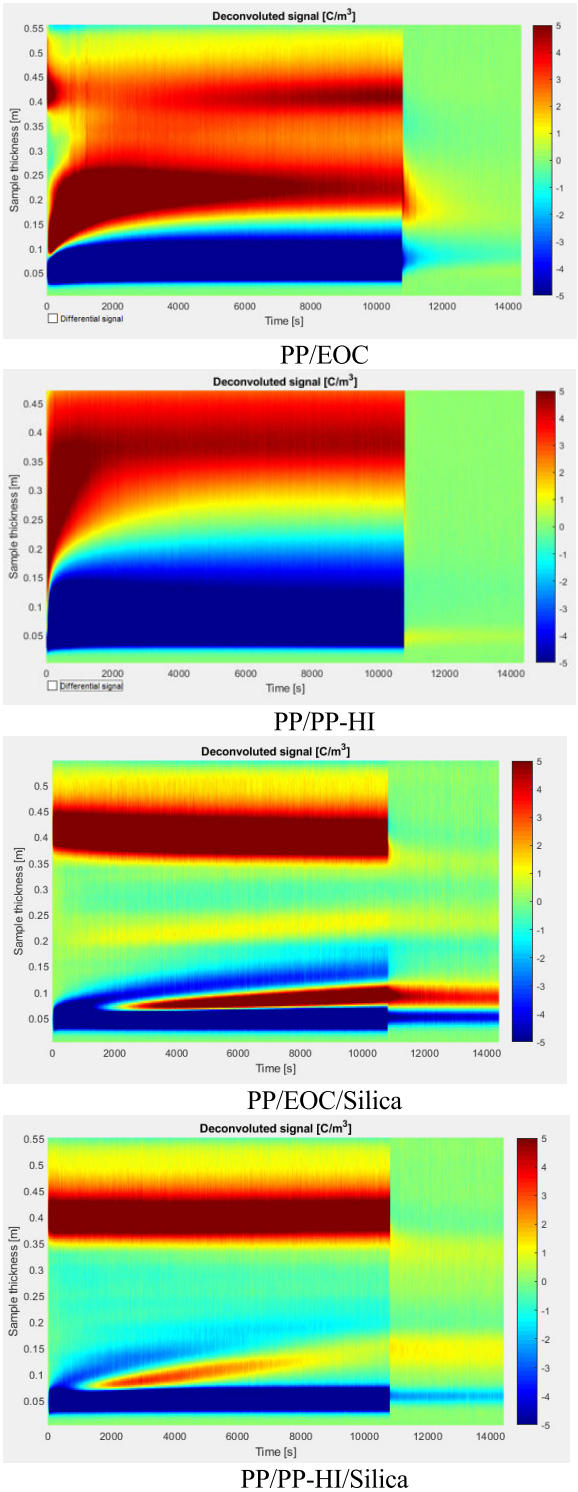

FIGURE 13. Space charge profiles of PP/EOC, PP/PP-HI blends and PP/EOC/Silica, PP/PP-HI/Silica nanocomposites.

slightly lower than the one of PP/PP-HI (0.98eV), as shown in Figure 9. In general, deeper traps can hinder charge injection causing a reduction of it; therefore also trap density should be considered. The amount of charge is not only related to the trap depth, but also to trap density. Trap density for the PP/EOC sample is higher than for the PP/PP-HI

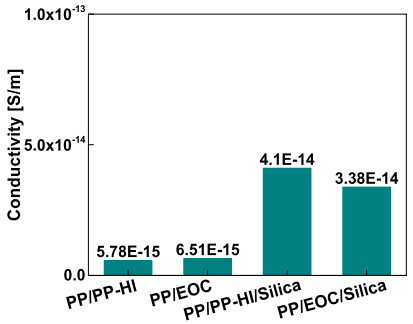

FIGURE 14. Conductivity of the PP/EOC, PP/PP-HI blends and the PP/EOC/Silica, PP/PP-HI/Silica nanocomposites.

sample, and this can actually result in a higher degree of charge injection, despite of a deeper trap level. Additionally, the charge injection is also related to the temperature (the poling phase is 70 °C and 60 °C for TSDC and PEA, respectively) and electric field (3 kV and 30 kV for TSDC and PEA, respectively). The amount of space charge is a sum of these complex factors.

The addition of silica significantly decreases the presence of charge packets and reduces the amount of heterocharges trapped near the cathode, as shown in the bottom part of Figure 13. Table 3 also shows that addition of nanosilica decreases space charge accumulation of the PP/EOC and PP/PP-HI blends.

Furthermore, focus should be put on the depolarization phase of space charge profiles in Figure 13. The experimental results confirm what was observed from TSDC measurements as shown in Figure 8 for both, the unfilled blends as well as the composites. Charges generally deplete slower in the nanocomposites than in the unfilled blends due to the presence of deep charge traps introduced by the addition of silica. Materials featuring deeper traps can be considered as not suitable for HVDC cable applications, since the charge storage can result in maintaining the field deformation induced by space charge, in case the latter is accumulated for longer times, leading to faster degradation of the insulating material [36]. However, in our case, the overall lower amount of space charge accumulation can counterbalance the effect of slower charge depletion. Thus, overall improvement of the long term dielectric performance for this material can be expected.

I. CONDUCTIVITY

The conductivity test was performed at elevated temperature (60 °C) under an electric field of 30 kV/mm, and the results are shown in Figure 14. It should be noted that those results are arising from measurements taken after the polarization current reached full steady state.

Previously it was discussed that the addition of silica could decrease the conductivity of polymer nanodielectrics due to lower charge mobility resulting from the introduction of deeper traps. However, the opposite effect was observed in this study. The addition of the silica resulted in a higher conductivity than the unfilled blends exhibit. This result can be explained by electrical conduction processes being closely related to the motion of polymer chains [37]. In our case, adding nanosilica decreases the crystallinity of the polymer matrix, resulting in a higher amount of amorphous chains in the nanocomposites. These chains are more mobile. Consequently, the conductivity of the nanocomposites is slightly higher than the one of the unfilled blends.

IV. CONCLUSION

The morphological, mechanical and dielectric properties of PP/EOC and PP/PP-HI blends as well as PP/EOC/Silica and PP/PP-HI/Silica nanocomposites were studied. SEM images showed that there is a co-continuous phase separation in the PP/EOC blend, while only one smooth phase in PP/PP-HI blend was visible. This shows that PP and EOC have a significantly lower miscibility than PP and PP-HI. It consequently leads to two melting and two crystallization peaks in the PP/EOC and PP/EOC/Silica samples, while only one melting and crystallization peak in the PP/PP-HI and PP/PP-HI/Silica samples were recorded. The nanosilica was selectively located in the PP phase in the PP/EOC/Silica composite, but evenly dispersed in the whole matrix of the PP/PP-HI/Silica. TGA results showed that the thermal weight loss of PP/PP-HI is lower at a certain temperature than of the loss of the PP/EOC blend. Adding nanosilica increase the thermal stability of both polymer blends. The crystallinity and storage modulus of the PP/EOC blend are higher compared to the PP/PP-HI material, as shown by DSC and DMA results, respectively. The addition of nanosilica resulted in a decrease in both, crystallinity and storage modulus of the polymer blends.

The DSC results showed that the nanosilica acts as nucleating agent, which increased the crystallization temperature of both polymer blends. DMA curves presented three different polymer transition peaks: β (glass transition), $\alpha 1$ (crystal rearrangement) and $\alpha 2$ (melting) transition peaks. The addition of nanosilica did not affect the polymer transition peak position. TSDC results showed that the trap density of the PP/EOC blend is higher than the one of PP/PP-HI, and that the trap depth of PP/EOC is deeper compared to PP/PP-HI. Nanosilica can introduce deep traps in both polymer blends and decrease the space charge accumulation shown by PEA results. However, the presence of nanosilica increased the conductivity of both polymer blends. Overall, the PP/PP-HI blend exhibited better performance than the PP/EOC blend. PP/PP-HI filled with 2% of APTES modified silica nanocomposite showed a potential for PP based HVDC cable insulation application in terms of decreased space charge accumulation.

ACKNOWLEDGMENT

This project has received funding from the European Union's Horizon 2020 research and innovation program under grant agreement No 720858. The authors also would like to thank Evonik Industries for providing a free silica sample.

REFERENCES

[1] Y. Zhou, B. Dang, H. Wang, J. Liu, Q. Li, J. Hu, and J. He, "Polypropylene-based ternary nanocomposites for recyclable high-voltage direct-current cable insulation," *Compos. Sci. Technol.*, vol. 165, pp. 168–174, Sep. 2018.

[2] Y. Gao, J. Li, Y. Yuan, S. Huang, and B. Du, "Trap distribution and dielectric breakdown of isotactic polypropylene/propylene based elastomer with improved flexibility for DC cable insulation," *IEEE Access*, vol. 6, pp. 58645–58661, 2018.

[3] X. Huang, J. Zhang, P. Jiang, and T. Tanaka, "Material progress toward recyclable insulation of power cables part 2: Polypropylene-based thermoplastic materials," *IEEE Elect. Insul. Mag.*, vol. 36, no. 1, pp. 8–18, Jan. 2020.

[4] P. Meng, Y. Zhou, C. Yuan, Q. Li, J. Liu, H. Wang, J. Hu, and J. He, "Comparisons of different polypropylene copolymers as potential recyclable HVDC cable insulation materials," *IEEE Trans. Dielectr. Electr. Insul.*, vol. 26, no. 3, pp. 674–680, Jun. 2019.

[5] I. L. Hosier, L. Cozzarini, A. S. Vaughan, and S. G. Swingler, "Propylene based systems for high voltage cable insulation applications," in *Proc. J. Phys., Conf.*, vol. 183, Aug. 2009, Art. no. 012015.

[6] C. D. Green, A. S. Vaughan, G. C. Stevens, A. Pye, S. J. Sutton, T. Geussens, and M. J. Fairhurst, "Thermoplastic cable insulation comprising a blend of isotactic polypropylene and a propylene-ethylene copolymer," *IEEE Trans. Dielectr. Electr. Insul.*, vol. 22, no. 2, pp. 639–648, Apr. 2015.

[7] B. Dang, J. He, J. Hu, and Y. Zhou, "Large improvement in trap level and space charge distribution of polypropylene by enhancing the crystalline-amorphous interface effect in blends," *Polym. Int.*, vol. 65, no. 4, pp. 371–379, 2016.

[8] G. N. Avgeropoulos, F. C. Weissert, P. H. Biddison, and G. G. A. Bohm, "Heterogeneous blends of polymers. Rheology and morphology," *Rubber Chem. Technol.*, vol. 49, no. 1, pp. 93–104, Mar. 1976.

[9] Y. Gao, J. Li, T. Han, Y. Yuan, S. Huang, and Y. Liu, "Temperature and trap distribution dependence of electrical tree growth characteristics in polypropylene/elastomer blends for recyclable cable insulation," *IET Sci., Meas. Technol.*, vol. 13, no. 5, pp. 755–765, 2019.

[10] Y. Zhou, J. He, J. Hu, and B. Dang, "Surface-modified MgO nanoparticle enhances the mechanical and direct-current electrical characteristics of polypropylene/polyolefin elastomer nanodielectrics," *J. Appl. Polym. Sci.*, vol. 133, no. 1, p. 42863, Jan. 2016.

[11] X. He, I. Rytöluoto, R. Anyszka, A. Mahtabani, E. Saarimäki, K. Lahti, M. Paajanen, W. Dierkes, and A. Blume, "Surface modification of fumed silica by plasma polymerization of acetylene for PP/POE blends dielectric nanocomposites," *Polymers*, vol. 11, no. 12, p. 1957, Nov. 2019.

[12] B. X. Du, Z. H. Hou, Z. L. Li, and J. Li, "Temperature dependent space charge and breakdown strength of PP/ULDPE/graphene nanocomposites for HVDC extruded cable insulation," *IEEE Trans. Dielectr. Electr. Insul.*, vol. 26, no. 3, pp. 876–884, Jun. 2019.

[13] Y. Zare and H. Garmabi, "Nonisothermal crystallization and melting behavior of PP/nanoclay/$CaCO_3$ ternary nanocomposite," *J. Appl. Polym. Sci.*, vol. 124, no. 2, pp. 1225–1233, Apr. 2012.

[14] F. M. Mirabella and A. Bafna, "Determination of the crystallinity of polyethylene/α-olefin copolymers by thermal analysis: Relationship of the heat of fusion of 100% polyethylene crystal and the density," *J. Polym. Sci. B, Polym. Phys.*, vol. 40, no. 15, pp. 1637–1643, Aug. 2002.

[15] J. Ying, S. Liu, F. Guo, X. Zhou, and X. Xie, "Non-isothermal crystallization and crystalline structure of PP/POE blends," *J. Thermal Anal. Calorimetry*, vol. 91, no. 3, pp. 723–731, 2008.

[16] B. Dang, Q. Li, Y. Zhou, J. Hu, and J. He, "Suppression of elevated temperature space charge accumulation in polypropylene/elastomer blends by deep traps induced by surface-modified ZnO nanoparticles," *Compos. Sci. Technol.*, vol. 153, pp. 103–110, Dec. 2017.

[17] K. Chrissafis, K. M. Paraskevopoulos, E. Pavlidou, and D. Bikiaris, "Thermal degradation mechanism of HDPE nanocomposites containing fumed silica nanoparticles," *Thermochimica Acta*, vol. 485, nos. 1–2, pp. 65–71, Mar. 2009.

[18] Q. Jiasheng and H. Pingsheng, "Non-isothermal crystallization of HDPE/nano-SiO_2 composite," *J. Mater. Sci.*, vol. 38, no. 11, pp. 2299–2304, 2003.

[19] T. G. Gopakumar, J. A. Lee, M. Kontopoulou, and J. S. Parent, "Influence of clay exfoliation on the physical properties of montmorillonite/polyethylene composites," *Polymer*, vol. 43, no. 20, pp. 5483–5491, 2002.

[20] R. R. Babu, N. K. Singha, and K. Naskar, "Effects of mixing sequence on peroxide cured polypropylene (PP)/ethylene octene copolymer (EOC) thermoplastic vulcanizates (TPVs). Part. I. Morphological, mechanical and thermal properties," *J. Polym. Res.*, vol. 17, no. 5, pp. 657–671, 2010.

[21] B. Wang and H. X. Huang, "Effects of halloysite nanotube orientation on crystallization and thermal stability of polypropylene nanocomposites," *Polym. Degradation Stability*, vol. 98, no. 9, pp. 1601–1608, 2013.

[22] L. Jw, A. Hassan, R. Ar, and W. Mu, "Morphology, thermal and mechanical behavior of polypropylene nanocomposites toughened with poly (ethylene co octene)," *Polym. Int.*, vol. 55, no. 2, pp. 204–215, 2006.

[23] N. S. Allen and M. Edge, *Fundamentals of Polymer Degradation and Stabilization*. Cham, Switzerland: Springer, 1992, p. 5.

[24] K. Chrissafis, K. M. Paraskevopoulos, S. Y. Stavrev, A. Docoslis, A. Vassiliou, and D. N. Bikiaris, "Characterization and thermal degradation mechanism of isotactic polypropylene/carbon black nanocomposites," *Thermochimica Acta*, vol. 465, nos. 1–2, pp. 6–17, Dec. 2007.

[25] M. Zanetti, G. Camino, P. Reichert, and R. Mülhaupt, "Thermal behaviour of poly (propylene) layered silicate nanocomposites," *Macromol. Rapid Commun.*, vol. 22, no. 3, pp. 176–180, 2001.

[26] N. L. Batista, P. Olivier, G. Bernhart, M. C. Rezende, and E. C. Botelho, "Correlation between degree of crystallinity, morphology and mechanical properties of PPS/carbon fiber laminates," *Mater. Res.*, vol. 19, no. 1, pp. 195–201, Feb. 2016.

[27] S. Dai, L. Ye, and G. Hu, "Preparation and properties of PP/PC/POE blends," *Polym. Adv. Technol.*, vol. 21, no. 4, pp. 279–289, 2010.

[28] H.-Y. Tsi, W.-C. Tsen, Y.-C. Shu, F.-S. Chuang, and C.-C. Chen, "Compatibility and characteristics of poly(butylene succinate) and propylene-co-ethylene copolymer blend," *Polym. Test.*, vol. 28, no. 8, pp. 875–885, Dec. 2009.

[29] J.-R. Yi, X.-L. Xi, X.-P. Zh, H.-M. Zh, and D.-Q. Li, "Dynamic mechanical behavior and prediction for PP/POE blends," *Chem. Res. Chin. Univ.*, vol. 25, no. 4, pp. 573–578, 2009.

[30] S. Mohanty and S. K. Nayak, "Dynamic-mechanical and thermal characterization of polypropylene/ethylene–octene copolymer blend," *J. Appl. Polym. Sci.*, vol. 104, no. 5, pp. 3137–3144, Jun. 2007.

[31] A. S. Luyt, M. D. Dramicanin, Ž. Antic, and V. Djokovic, "Morphology, mechanical and thermal properties of composites of polypropylene and nanostructured wollastonite filler," *Polym. Testing*, vol. 28, no. 3, pp. 348–356, 2009.

[32] R. H. Boyd, "Relaxation processes in crystalline polymers: Experimental behaviour—A review," *Polymer*, vol. 26, no. 3, pp. 323–347, 1985.

[33] X. Wang, H. Q. He, D. M. Tu, C. Lei, and Q. G. Du, "Dielectric properties and crystalline morphology of low density polyethylene blended with metallocene catalyzed polyethylene," *IEEE Trans. Dielectr. Electr. Insul.*, vol. 15, no. 2, pp. 319–326, Apr. 2008.

[34] B. X. Du, H. Xu, J. Li, and Z. Li, "Space charge behaviors of PP/POE/ZnO nanocomposites for HVDC cables," *IEEE Trans. Dielectr. Electr. Insul.*, vol. 23, no. 5, pp. 3165–3174, Oct. 2016.

[35] X. He, I. Rytoluoto, R. Anyszka, A. Mahtabani, E. Saarimaki, K. Lahti, M. Paajanen, W. Dierkes, and A. Blume, "Silica surface-modification for tailoring the charge trapping properties of PP/POE based dielectric nanocomposites for HVDC cable application," *IEEE Access*, vol. 8, pp. 87719–87734, 2020.

[36] D. Ma, T. A. Hugener, R. W. Siegel, A. Christerson, E. Mårtensson, C. Önneby, and L. S. Schadler, "Influence of nanoparticle surface modification on the electrical behaviour of polyethylene nanocomposites," *Nanotechnology*, vol. 16, no. 6, p. 724, 2005.

[37] C. Zhang, J.-W. Zha, H.-D. Yan, W.-K. Li, Y.-Q. Wen, and Z.-M. Dang, "Effects of trap density on space charge suppression of block polypropylene/AI_2O_3 composite under high temperature," *IEEE Trans. Dielectr. Electr. Insul.*, vol. 25, no. 4, pp. 1293–1299, Aug. 2018.

[38] M. Gao, J. Yang, H. Zhao, H. He, M. Hu, and S. Xie, "Preparation methods of polypropylene/nano-silica/styrene-ethylene-butylene-styrene composite and its effect on electrical properties," *Polymers*, vol. 11, no. 5, p. 797, May 2019.

[39] F. Saiz and N. Quirke, "The excess electron in polymer nanocomposites," *Phys. Chem. Chem. Phys.*, vol. 20, no. 43, pp. 27528–27538, Nov. 2018.

[40] Y. Zhou, C. Yuan, C. Li, P. Meng, J. Hu, Q. Li, and J. He, "Temperature dependent electrical properties of thermoplastic polypropylene nanocomposites for HVDC cable insulation," *IEEE Trans. Dielectr. Electr. Insul.*, vol. 26, no. 5, pp. 1596–1604, Oct. 2019.

[41] Y. Gao, J. Li, Y. Li, Y. Q. Yuan, S. H. Huang, and B. X. Du, "Effect of elastomer type on electrical and mechanical properties of polypropylene/elastomer blends," in *Proc. Int. Symp. Electr. Insul. Mater. (ISEIM)*, Toyohashi, Japan, Sep. 2017, pp. 574–577.

XIAOZHEN HE (Member, IEEE) was born in Yantai, Shandong, China, in 1990. She received the M.Sc. degree in polymer chemistry and physics from the Qingdao University Science and Technology, China, in 2017.

She joined the Elastomer Technology and Engineering Group, University of Twente, Enschede, The Netherlands, as a Ph.D. Student, in 2017. She is currently working on the EU Project GRIDABLE. The aim of this project is to develop novel dielectric thermoplastic polymer composite materials for HVDC cable and DC capacitors application. In this project, she is responsible for the nanofiller surface modification via solvent free method and plasma technology. Her research interests include HVDC cable insulation material, nanocompsosites, nanofiller surface engineering, and thermoplastic, rubber, and plasma technology.

PAOLO SERI (Member, IEEE) was born in Macerata, Italy, in June 1986. He received the master's degree in energy engineering and the Ph.D. degree in electrical engineering from the University of Bologna, in 2012 and 2016, respectively. Since 2017, he has been a part of the Laboratory of Innovative Materials for Electrical Systems (LIMES), University of Bologna, as a Research Fellow, currently working on the topics of HVDC cables design, partial discharge detection and modeling, and characterization of dielectric materials. He is also an Assistant Professor with the Department of Electrical, Electronic and Information Engineering (DEI), Bologna University.

ILKKA RYTÖLUOTO received the M.Sc. (Tech.) and Ph.D. degrees in electrical engineering from Tampere University (TAU), Tampere, Finland, in 2011 and 2016, respectively. From 2011 to 2019, he was with the High Voltage Engineering research group, TAU, and since 2019, he has been working as a Senior Scientist with the VTT Technical Research of Center of Finland. He has more than ten years of experience in the field of high voltage engineering and dielectric material development, especially in thin biaxially oriented capacitor films and HVDC cable insulation, and several years of experience in polymers processing and characterization. His current research interests include polypropylene-based dielectric nanocomposites for high-voltage DC film capacitors and cables, processing-morphology-electrical property relationships of dielectric and electrically conductive polymeric systems, functional polymer composites, polymer processing and recycling, and biaxially oriented thin film technology.

RAFAL ANYSZKA (Member, IEEE) received the master's degree from the Lodz University of Technology, Poland, in 2010. Afterwards, he continued Ph.D. studies at the Lodz University of Technology conducting research in the field of ceramizable elastomer composites. In 2014, he defended his Ph.D. thesis and started a two years project at his Alma mater concerning the development of sulphur-organic co-polymers and composites on their base. From 2017 to 2018, he was working as a Postdoctoral Researcher with the University of Twente developing hook-and-loop molecular adhesive systems for new generation elastomers. In 2018, he joined the European GRIDABLE project focused on silica surface modification for high voltage DC recyclable insulation materials.

AMIRHOSSEIN MAHTABANI (Member, IEEE) received the B.Sc. degree in polymer engineering from the University of Tehran, Iran, in 2013, and the M.Sc. degree in polymer engineering from Tarbiat Modares University, Iran, in 2015. He is currently pursuing the Ph.D. degree with the University of Twente. He is also the Chair of the Elastomer Technology and Engineering Group, University of Twente. His research interests include nanoparticle modification, nanocomposite development, interface engineering, and fabrication of nanostructured surfaces.

HADI NADERIALLAF (Member, IEEE) was born in Mashhad, Iran, in April 1986. He received the M.Sc. degree in electrical engineering from the Leibniz Universität Hannover, Germany, in 2012. He is currently pursuing the Ph.D. degree with the University of Bologna, Italy, working on the EU project GRIDABLE. He did his master thesis at the Schering Institute of High Voltage Techniques and Engineering, Leibniz Universität Hannover. He has working experience for five years as a Transformer Fluid Specialist. His research interests include liquid and nanostructured solid electrical insulating materials, HVDC cables design, space charge measurement and analysis, AC and DC partial discharge detection and modeling, insulation systems for electrical machines, condition monitoring techniques, HV transformer asset management, and DGA and transformer oil reclamation.

MINNA NIITTYMÄKI (Graduate Student Member, IEEE) received the M.Sc. (Tech.) degree in electrical engineering from the Tampere University of Technology, in 2012. Since then, she has been working as a Researcher with the High Voltage Engineering research group, TUT (since 2019 known as Tampere University (TAU)), with the aim towards Ph.D. degree. She has over eight years of experience in the field of high voltage engineering and dielectric material development. Her current research interests include insulation systems focusing on the dielectric characterization of nanocomposite polymer materials and thermally sprayed insulating ceramic coatings.

EETTA SAARIMÄKI received the M.Sc. (Tech.) degree in plastics technology from the Tampere University of Technology, Tampere, Finland, in 1993. She worked with the VTT Technical Research Center of Finland Ltd., since 1994 and is currently working as a Senior Scientist. Her research interests include plastic processing technologies (especially extrusion, compounding, and orientation), electromechanical films, plastic nanocomposites, functional polymer composites, electrical insulation materials, and plastics recycling.

CHRISTELLE MAZEL received the Ph.D. degree in ceramic materials from the Laboratoire de Science des Procédés Céramiques et Traitements de Surface (SPCTS - UMR 6638), University of Limoges, in 2001.

She was an Engineer of ceramic materials science with the Ecole Nationale Supérieure de Ceramique Industrielle, Limoges, France, in 1997. She started her industrial career in 2001 as a Product Development Engineer at Alcatel Cable with the development of the INFIT insulation technology for fire resistance cables. In 2011, she joined the HV-MV systems team and was involved in the development of POWERBOOST insulation system. Her research interests include the polymer formulation work (insulation and semiconductive materials for power cables), their processing, and their characterizations (physico-chemical, thermomechanical, rheological, and electrical properties).

GABRIELE PEREGO received the Ph.D. degree in organic chemistry from the Università degli Studi di Torino. He has been working over 30 years in field of polymeric materials. He is currently a Scientific Director with Nexans Research Center. He worked as a Project Manager for HVDC extruded cables and accessories from basic investigations up to HV and EHV qualification. He has acted also as a Project Manager for the development of PP based thermoplastic cable technology for both AC and DC applications.

KARI LAHTI (Member, IEEE) received the M.Sc. and Ph.D. degrees in electrical engineering from the Tampere University of Technology, in 1994 and 2003, respectively. He has over 25 years of experience in the field of high voltage engineering. Since 2003, he has been responsible of the High Voltage Laboratory of TUT (since 2019 known as Tampere University (TAU)) and since 2013, he has also been the Head of the TAU's research group on High Voltage Engineering, focusing mainly on various aspects of high voltage insulation systems. He currently holds the position of Senior Scientist/Adjunct Professor with the Tampere University of Technology. His research interests include high voltage metrology and testing techniques, surge arresters, nanocomposite insulation systems, and environmental testing of HV apparatus and dielectric characterization of HV insulation systems.

MIKA PAAJANEN received the M.Sc. (Tech.) and D.Sc. (Tech.) degrees in electrical engineering and technical physics from the Tampere University of Technology, in 1995 and 2001, respectively. He worked with the VTT Technical Research Center of Finland Ltd., since 1996 and is currently working as a Principal Scientist. His research interests include electromechanical films, electrets, plastic nanocomposites, electrical insulation materials, and plastics recycling.

WILMA DIERKES studied chemistry at the Technical University in Hanover, Germany. She continued with a postgraduate study in environmental science at the Fondation Universitaire Luxembourgeoise, Arlon, Belgium. After finishing this study, she started working for the rubber recycling company Rubber Resources in Maastricht, the Netherlands. She was in charge of Research and Development and Technical Service, and developed and introduced short recycling loops for production waste back into the original production process. The next step in her career was the Research and Development Department of Robert Bosch Produktie, Tienen, Belgium, where she developed windshield wipers. Additionally, she was the Head of the Chemical Laboratory and part of the trouble shooting team in the production facility. In 2001, she started to work for the University of Twente, Enschede. From 2009 till 2013, she also held a part-time professorship at the Tampere Technical University, Finland. Her research interests include reinforcing filler technology, with emphasis on silica filler systems, and recycling and re-utilization of elastomers. Other research areas are polymer networks and fiber reinforcement. Since, she started her research work at the university, she published more than 100 reviewed articles, 12 book chapters, and she holds eight patents. For about ten years, she was a board member of the Dutch Association of Plastics and Rubber Technologists (VKRT), and from 2005 till 2014, she was the Chairman of this association.

ANKE BLUME studied chemistry at the University of Hanover, Germany, in October 1988 until July 1993. In the last year of her study, she came in the first contact with rubber during her master thesis. Consequently, she carried out her Ph.D. thesis at the "German Institute for Rubber Technology" (DIK) which she finished mid of November 1995. After nine months postdoc time at the DIK, she started in September 1996 as a member of the product development group silica in the Applied Technology Department of Degussa AG. She worked there in different positions, always related to the development of silica and silane for the use in rubber. Degussa changed several times the name, currently it is "Evonik Resource Efficiency GmbH." Since August 2011, she has the position as an "IP Manager silica and silane for rubber applications." In October 2013, she started at the University of Twente, The Netherlands, as the Head of the Chair "Elastomer Technology and Engineering (ETE)" Group.